Global Change Biology (2004) **10,** 1767–1784, doi: 10.1111/j.1365-2486.2004.00837.x

Associations between carbon isotope ratios of ecosystem respiration, water availability and canopy conductance

N. G. MCDOWELL*, D. R. BOWLING†, A. SCHAUER†, J. IRVINE‡, B. J. BOND‡, B. E. LAW‡, AND J. R. EHLERINGER†

*Earth and Environmental Sciences Division, Los Alamos National Laboratory, MS-D462 Los Alamos, NM 87545, USA, †Stable Isotope Ratio Facility for Environmental Research, Department of Biology, University of Utah, 257 South 1400 East, Salt Lake City, UT 84112, USA, ‡Department of Forest Science, College of Forestry, Oregon State University, Corvallis, OR 97331, USA

Abstract

We tested the hypothesis that the stable carbon isotope signature of ecosystem respiration ($\delta^{13}C_R$) was regulated by canopy conductance (G_c) using weekly Keeling plots ($n = 51$) from a semiarid old-growth ponderosa pine (*Pinus ponderosa*) forest in Oregon, USA. For a comparison of forests in two contrasting climates we also evaluated trends in $\delta^{13}C_R$ from a wet 20-year-old Douglas-fir (*Pseudotsuga menziesii*) plantation located near the Pacific Ocean. Intraannual variability in $\delta^{13}C_R$ was greater than 8.0‰ at both sites, was highest during autumn, winter, and spring when rainfall was abundant, and lowest during summer drought. The $\delta^{13}C_R$ of the dry pine forest was consistently more positive than the wetter Douglas-fir forest (mean annual $\delta^{13}C_R$: −25.41‰ vs. −26.23‰, respectively, $P = 0.07$). At the Douglas-fir forest, $\delta^{13}C_R$–climate relationships were consistent with predictions based on stomatal regulation of carbon isotope discrimination (Δ). Soil water content (*SWC*) and vapor pressure deficit (*vpd*) were the most important factors governing $\delta^{13}C_R$ in this forest throughout the year. In contrast, $\delta^{13}C_R$ at the pine forest was relatively insensitive to *SWC* or *vpd*, and exhibited a smaller drought-related enrichment (~2‰) than the enrichment observed during drought at the Douglas-fir forest (~5‰). Groundwater access at the pine forest may buffer canopy–gas exchange from drought. Despite this potential buffering, $\delta^{13}C_R$ at the pine forest was significantly but weakly related to canopy conductance (G_c), suggesting that $\delta^{13}C_R$ remains coupled to canopy–gas exchange despite groundwater access. During drought, $\delta^{13}C_R$ was strongly correlated with soil temperature at both forests. The hypothesis that canopy-level physiology is a critical regulator of $\delta^{13}C_R$ was supported; however, belowground respiration may become more important during rain-free periods.

Keywords: carbon isotopes, climate, ecosystem respiration, Keeling plot, *Pinus ponderosa*, *Pseudotsuga menziesii*, stomatal conductance

Received 27 February 2004; received and accepted 27 April 2004

Introduction

Rising CO_2 concentrations and the subsequent concern regarding greenhouse gas-induced climate change has been a driving force for the development of new techniques to estimate the global carbon budget (Canadell *et al.*, 2000). One technique that is seeing increased use is isotopic mass-balance models (Tans, 1980; Ciais *et al.*, 1995; Fung *et al.*, 1997; Battle *et al.*, 2000; Randerson *et al.*, 2002a). This technique capitalizes on the seasonal oscillations in $\delta^{13}C$ of atmospheric CO_2 that are driven in part by respired $\delta^{13}C$ from terrestrial ecosystems ($\delta^{13}C_R$, Flanagan & Ehleringer, 1998). Accurate parameterization of models that predict seasonal and spatial variation in $\delta^{13}C_R$ is critical to the accuracy of terrestrial–oceanic sink partitioning estimates (Randerson *et al.*, 2002b); however, measurements of $\delta^{13}C_R$ are few and have often focused on seasons favorable for field work, i.e., the Northern Hemisphere summer.

One popular method to model $\delta^{13}C_R$ is a bottom-up approach in which we employ our knowledge of the controls over *leaf-level* carbon isotope discrimination (Δ)

Correspondence: N. G. McDowell, tel. +1 505 665 2909, fax +1 505 665 3285, e-mail: mcdowell@lanl.gov

and the subsequent $\delta^{13}C$ of plant organic matter (Lloyd & Farquhar, 1994). These well-known leaf-level mechanisms also provide useful working hypotheses regarding controls over ecosystem scale Δ and subsequent $\delta^{13}C_R$.

Photosynthesis by terrestrial C_3 plants discriminates against $^{13}CO_2$ relative to $^{12}CO_2$ because $^{13}CO_2$ has a lower diffusivity through the stomatal pore and lower affinity with the carboxylating enzyme Rubisco (ribulose 1,5-bisphosphate carboxylase-oxygenase). Discrimination results in a decrease in $\delta^{13}C$ of plant matter of approximately 20‰ below that of atmospheric CO_2. Discrimination and the resulting $\delta^{13}C$ signature of photosynthate can be expressed mathematically as (Farquhar *et al.*, 1989)

$$\delta^{13}C \approx \delta^{13}C_a - a - (b - a)\frac{c_i}{c_a}. \qquad (1)$$

In this simplified equation, $\delta^{13}C_a$ is the isotopic composition of source air used in photosynthesis, a is the fractionation associated with diffusion in air (4.4‰) and b is the net fractionation associated with carboxylation by Rubisco (27–29‰), and c_i and c_a are the intercellular and atmospheric partial pressures of CO_2, respectively. There is a physiological link between Δ and gas exchange because stomatal conductance (g) and photosynthetic assimilation (A) regulate c_i:

$$c_i = c_a - \frac{A}{g}, \qquad (2)$$

where A/g is also referred to as the intrinsic water use efficiency (Ehleringer, 1993). Changes in A/g cause a proportional change in the $\delta^{13}C$ of photosynthate. For example, increases in A such as because of increased light availability typically result in more positive values of $\delta^{13}C$ of photosynthetic products, and increases in g such as because of increased soil or atmospheric water content tend to result in more negative values of $\delta^{13}C$.

In theory, we should be able to model $\delta^{13}C_R$ using Eqns (1) and (2) if canopy-scale photosynthetic discrimination influences $\delta^{13}C_R$. The $\delta^{13}C$ of carbohydrates results directly from Δ (Brugnoli *et al.*, 1998; Brugnoli & Farquhar, 2000) and should translate to $\delta^{13}C$ of respiration since there is no fractionation during cellular respiration (Lin & Ehleringerm 1997), although metabolic fractionation (Ghashgaie *et al.*, 2003) and ecosystem-scale disequilibrium (Schnyder *et al.*, 2003) introduce extra factors into the gas exchange–$\delta^{13}C_R$ relationship. Nonetheless, carbon transport from assimilation to respiration appears to be rapid ($\leq$10 days, Ekblad & Högberg, 2001; Högberg *et al.*, 2001; Bowling *et al.*, 2002; Bhupinderpal Singh *et al.*, 2003). Indeed, an emerging pattern in ecosystem-scale studies is that $\delta^{13}C_R$ often (but not always) responds to environmental factors in a manner consistent with Eqns (1) and (2). A summary by Buchmann *et al.* (1998) concluded that significant differences in $\delta^{13}C$ exist between evergreen and deciduous forests, with regard to stand structure and site history (C_3 vs. C_4 plants). These differences are consistent with Eqns (1) and (2); however, very little seasonal variability was observed and environmental drivers were not identified. This was due in part to the sampling constraints imposed by sample-processing limitations during the 1990s. Since then technological advancements have allowed increased sample frequency (Ehleringer & Cook, 1998; Schauer *et al.*, 2003) and subsequently, ecosystem water balance has emerged as a common factor regulating $\delta^{13}C_R$. Fessenden & Ehleringer (2003) and Lai *et al.* (2004) observed significant negative relationships between $\delta^{13}C_R$ and soil water content (*SWC*), Ometto *et al.* (2002) found $\delta^{13}C_R$ was coupled to monthly precipitation, and Bowling *et al.* (2002) found $\delta^{13}C_R$ was positively related to atmospheric vapor pressure deficit (*vpd*) several days earlier (the shape of this relationship is shown in Fig. 1a). Each of these results is consistent with expectations of stomatal control over $\delta^{13}C_R$, and collectively they allow us to hypothesize that if stomatal regulation of Δ were the *dominant* factor controlling $\delta^{13}C_R$, then we should observe the general pattern shown in Fig. 1b. We use G_c rather than g to represent canopy conductance to be consistent with the measurement scale of $\delta^{13}C_R$ and because G_c includes boundary layer conductance (which may influence $\delta^{13}C_R$) and g does not.

The hypothesis embodied by Fig. 1b ignores the potentially large role of changes in the age (and associated $\delta^{13}C$) of carbon respired by heterotrophic respiration (Schönwitz *et al.*, 1986; Ciais *et al.*, 1999), changes in relative rates of respiration from different ecosystem components (e.g. above vs. belowground or roots vs. heterotrophs), changes in photosynthetic rates and subsequent effects on c_i/c_a (Eqn (2)) or other confounding factors. These factors could cause variation in $\delta^{13}C_R$ that overwhelm, or obscure detection of G_c effects on $\delta^{13}C_R$. For example, over a 2-week period of nightly sampling at a pine forest, we observed only a weak relationship between G_c and $\delta^{13}C_R$ (McDowell *et al.*, 2004). Freezing air temperatures occurred at the beginning of the sample period that has been implicated as a mechanism of stomatal closure and subsequent enriched $\delta^{13}C_R$ (Bowling *et al.*, 2002), however, G_c was insensitive to the freeze in our study (McDowell *et al.*, 2004), refuting that hypothesis. This indicates that the relationship between G_c and $\delta^{13}C_R$ may have been weak because of noncanopy controls on $\delta^{13}C_R$ such as belowground respiration.

A common limitation of $\delta^{13}C_R$ studies is the lack of long-term, continuous data sets that span all seasons and weather conditions. Indeed, most sampling has

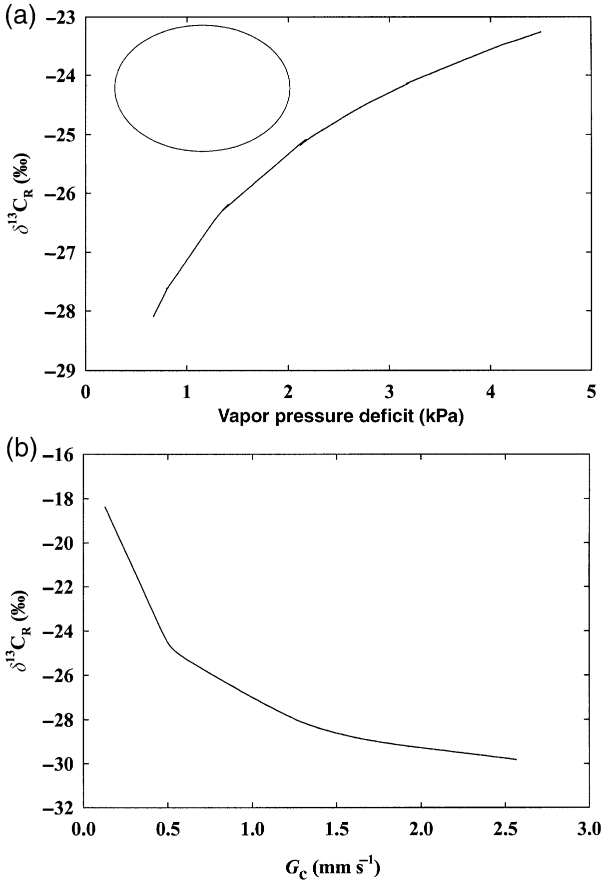

Fig. 1 (a) The relationship between $\delta^{13}C_R$ and vapor pressure deficit (*vpd*) and freezing air temperatures. The *vpd* trace and the circled area that represents $\delta^{13}C_R$ observed after freeze events are from Bowling *et al.* (2002). (b) Expected response of $\delta^{13}C_R$ to increasing canopy-scale stomatal conductance (G_c). The line was modeled with Eqns (1) and (2) assuming constant values for photosynthetic capacity and leaf temperature. The key point of this figure is not the absolute values but the shape of the curve.

been done during the 'summer' months, biasing the results towards that period, and limiting our knowledge of $\delta^{13}C_R$ during the other seasons. This hampers our ability to fully understand the controls over $\delta^{13}C_R$ and limits the knowledge base needed for $\delta^{13}C_R$ parameterization in isotopic mass balance models.

The primary goals of our experiment were the following: (1) to document weekly variation in $\delta^{13}C_R$ for a year from two coniferous forests with contrasting water availability, (2) to test the hypothesis that patterns in $\delta^{13}C_R$ observed at these forests during infrequent, summer sampling (shown in Fig. 1a) would continue to be observed with higher frequency throughout the year, and (3) to test the proximal mechanism behind the climate–$\delta^{13}C_R$ patterns; that G_c regulates $\delta^{13}C_R$ (shown in Fig. 1b). To meet these goals, we conducted weekly measurements of $\delta^{13}C_R$ at two sites representing extremely different climatic and age regimes; a young Douglas-fir (*Pseudotsuga menziesii*) plantation located in a mild and wet coastal environment and an old-growth ponderosa pine (*Pinus ponderosa*) forest located in a more extreme and dry continental climate. Hypothesis (3) was directly tested using sapflow-based estimates of G_c at the ponderosa pine forest. We recognized that nonstomatal, ecosystem-scale factors are also likely to influence $\delta^{13}C_R$ and therefore we also examined some $\delta^{13}C_R$–climate relationships, e.g., $\delta^{13}C_R$–soil temperature relationships.

Methods

Sites

The two forests used in this study are a 20-year-old Douglas-fir plantation located in western Oregon near the town of Blodgett (44°34N, 123°32W) and a ~250-year-old ponderosa pine forest located in the Metolius Research Natural Area near Sisters, Oregon (44°30N, 121°37W). The Douglas-fir forest is located at approximately 330 m elevation on a flat slope at the base of a gently sloping hill. The entire uphill slope and the flat area are dominated by Douglas-fir trees of the same age and genetic stock. A small component of western hemlock (*Tsuga heterophylla*) and red alder (*Alnus rubra*) was present and the understory vegetation was sparse and dominated by sword fern (*Polystichum munitum*) and salal (*Gaultheria shallon*). Leaf area index at similar, nearby sites is approximately 7.4 m^2 half surface area needles per m^2 ground (Weiskittel, 2003, R. H. Waring, personal communication). The climate at this site is characterized by wet but mildly cool winters and dry and warm summers, with an annual precipitation of approximately 1900 mm (Bowling *et al.*, 2002). This site has never been sampled for $\delta^{13}C_R$ before but it is located within 8 km of a Douglas-fir site of similar soils, stand age, genetic stock, and silvicultural treatment presented in Bowling *et al.* (2002). The ponderosa pine site is located at an elevation of 940 m on a nearly flat slope at the base of a ridge. Ponderosa pine-dominated forest extends for at least 12 km in all directions. The stand has two dominant age classes of trees consisting of ~250- and ~ 50-year-old trees, and a minor contribution (in regard to biomass) of saplings and seedlings of the same species. Understory vegetation is sparse. The canopy leaf area index is approximately 2.0 m^2 half surface area needles per m^2 ground (Law *et al.*, 1999). Climate at this site is characterized by warm, dry summers and wet, cool winters, with mean annual precipitation of 523 mm. This site is a member of the AmeriFlux network, and more extensive site details can be found in Law *et al.* (1999, 2001) and Anthoni *et al.* (2002). Previous $\delta^{13}C_R$ results from this site were presented in Ehleringer & Cook (1998), Bowling *et al.* (2002), and McDowell *et al.* (2004), and $\delta^{18}O_R$ results are presented in Bowling *et al.* (2003).

Micrometeorological data. We collected meteorological and micrometeorological measurements at half-hourly intervals at both forests. Measured parameters included air temperature (T_{air}), relative humidity, soil temperature (T_{soil}, at 2 and 15 cm depth in the ponderosa pine forest, and at 5 and 10 cm depths in the Douglas-fir forest), *SWC* (averaged over the top 30 cm depth at the ponderosa pine forest and over the top 15 cm at the Douglas-fir forest), photosynthetically active radiation (*PAR*), and above-canopy precipitation. Details of the meteorological measurements at the ponderosa pine forests are also described in Law *et al.* (2001). We also measured soil water potential (Ψ_s) at the pine forest via predawn measurements of leaf water potential of the 250-year-old pines using a Scholander-type pressure chamber (PMS, Corvallis, OR, USA). Values were corrected for the hydrostatic gradient (0.01 MPa m^{-1}). More details are provided in Irvine & Law (2002).

Automated sampling of atmospheric [CO$_2$] and δ^{13}C. We used automated sampling instruments to collect flask samples of air on a weekly basis at the two sites. The instrument design and sample integrity are described in detail by Schauer *et al.* (2003). Briefly, the instrument collects a total of fifteen 100 mL flask samples of air during a given night by pulling samples sequentially through flasks. During sampling, air is pulled from a filtered inlet through tubing, a valve manifold to select among different inlet lines, a magnesium perchlorate ($Mg(ClO_4)_2$) desiccating trap, a filter, a 16-position rotary valve, one of 15 glass flasks, an infrared gas analyzer (Li-800 Gas Hound, Li-Cor Inc., Lincoln, NE, USA), and a pump.

For this experiment, we programmed the samplers to collect a single flask from the span tank for assessment of system integrity, another two flasks during the middle of the afternoon, then 12 more flasks during the nocturnal period for the Keeling plots (described below). The [CO$_2$] in the canopy air space often has higher values close to the ground at night, and also, often increases at night because of respiration into a stable boundary layer. We take advantage of these vertical and temporal concentration gradients by drawing samples from a range of heights (depending on the forest) within the canopy air space throughout the night to ensure a range of concentrations for the Keeling plots. The sample inlet heights were 0.2, 0.8 and 11.4 m at the ponderosa pine forest, and 0.2, 0.8 and 8.0 m in the Douglas-fir forest. Sampling was programmed to begin 1 h after sunset and terminated prior to sunrise the following morning. The samplers fill each flask sequentially, switching from one flask to the next as [CO$_2$] changes sufficiently to ensure a large overall [CO$_2$] range for the Keeling plot (see Pataki *et al.*, 2003 for an explanation of the importance of large [CO$_2$] ranges for accurate Keeling plot intercepts). The sampler was programmed to obtain a minimum [CO$_2$] range depending on local conditions. This resulted in ranges from a minimum of 20 to $\geq$100 μmol mol^{-1}. The minimum range of 20 μmol mol^{-1} is a compromise between minimizing the standard error (SE) of the intercept and feasibility of obtaining the target [CO$_2$] range during windy or stormy periods, the latter of which is determined based on nocturnal field experience at these sites. If the minimum range was not met the autosampler discarded all flask samples and refilled them the following night. Because we usually visited the samplers every 7 days, we programmed the sampler to attempt five consecutive nights to meet the CO$_2$ range, 2 days after flasks were installed, allowing samples to reside for no more than five nights on the sampler. Uncertainties associated with samples residing over many days in the automated samplers are 0.8 μmol mol^{-1} for [CO$_2$] and 0.10‰ for δ^{13}C (Schauer *et al.*, 2003).

We conducted an assessment of automated sampler integrity for each sampling period by measurement of δ^{13}C and [CO$_2$] from a single flask collected from a premeasured tank of compressed air prior to each weekly set of flasks. Each night that flasks were filled, the automated sampler first filled a single flask with gas from a cylinder of compressed air. This particular flask was then measured and compared with previous measurements of the isotopic ratios and [CO$_2$] of that cylinder. For the pine sampler, four flasks (i.e., from 4 different days) had values that were deviated from cylinder values, and for the Douglas-fir sampler, two flasks indicated a deviation. In these cases, the test flask indicated that the system may have been leaky, which was typically because of fittings or valves being incompletely shut by the field operator. The Keeling plot intercepts (described below) estimated from those data sets were then examined in relation to environmental parameters, and were excluded from the final analyses if they were large outliers ($n = 2$ data sets from the pine forest, $n = 0$ from the Douglas-fir forest). We also excluded two data sets from the pine forest that were collected while snow covered the lower inlet. Estimates of $\delta^{13}C_R$ from these two nights were abnormally enriched, presumably because of sampling of CO$_2$ from within the snowpack. The CO$_2$

that resides within snowpacks may be up to 4.4‰ enriched relative to snow-surface efflux because of diffusional fractionation (Cerling *et al*., 1991).

Keeling plots for $\delta^{13}C_R$. We used the Keeling plot approach (Keeling, 1958) to assess the isotopic composition of CO_2 in respiratory fluxes. This approach uses a two-component mixing model that consists of the δ^{13}C of CO_2 respired from all organisms within the forest and δ^{13}C of CO_2 in the background atmosphere. The intercept of a linear regression of δ^{13}C of atmospheric CO_2 vs. $1/[CO_2]$ (where $[CO_2]$ is the mole fraction of CO_2) provides an estimate of $\delta^{13}C_R$. We used geometric mean (model II) regressions (Sokal & Rohlf, 1995). Uncertainties in the Keeling plot intercepts are expressed as SEs of the regression intercept. Outliers were assessed on each individual Keeling plot using a statistical approach in which any flask sample with a regression residual greater than two standard deviations of all the residuals on a given Keeling plot is removed. See Bowling *et al*. (2002) for more details on this approach. A total of 32 out of 1028 flasks were removed via this test (3%). We assumed no changes in δ^{13}C of the end-members during the sampling period for each individual Keeling plot. Our Keeling plot estimates are slightly more negative (0.003‰, results not shown) than if calculated using an alternative mixing model proposed by Miller & Tans (2003). See Pataki *et al*. (2003) for more details on the application of Keeling plots in ecosystem science.

Laboratory analyses. We measured carbon isotope ratios of flask samples on a continuous-flow isotope ratio mass spectrometer (IRMS; Finnigan MAT 252 or DELTAplus, San Jose, CA, USA) as described by Ehleringer & Cook (1998). Precision for δ^{13}C was determined daily by comparison with known standards and averaged 0.13‰ (Schauer *et al*., 2003). Corrections for the presence of ^{17}O were applied. CO_2 was separated from N_2O by gas chromatography before analysis. All δ^{13}C values are reported relative to the international Vienna Pee Dee Belemnite (VPDB) standard. Flask $[CO_2]$ was measured using the method of Bowling *et al*. (2001), and are traceable to the World Meteorological Organization CO_2 scale. Measurement precision was $\pm 0.2\,\mu mol\,mol^{-1}$.

Canopy stomatal conductance. Mean midday canopy conductance (G_c) was estimated at the ponderosa pine forest only. G_c was estimated with a simplified form of Penman–Monteith equation (Jarvis & McNaughton, 1986) where whole tree sap flux measurements averaged between 11:00 and 13:00 hours were used to determine canopy transpiration. See Irvine *et al*. (2002) for more details.

Statistical analyses. We conducted correlation analyses to examine relationships between $\delta^{13}C_R$ and factors such as *vpd*, cumulative *vpd* (defined as the sum of daily average *vpd* since the last rainfall event), T_{air}, T_{soil}, T_{min}, *PAR*, *SWC*, precipitation, cumulative precipitation and G_c. Daylight mean values of the factors were used unless specified otherwise. Because correlations between meteorological and physiological variables and respiratory fluxes may be lagged in time because of a delay between the time a given carbon atom is assimilated and respired, we conducted the correlations over a range of time lags (e.g. relationships between a climatic driving variable on day X and $\delta^{13}C_R$ on day $X + n$). To do this, we calculated averages of a given independent factor from 1 to 5 days, and then shifted these averages back in time by zero to 15 days (a subset of these results are reported in Tables 1–4). See Bowling *et al*. (2002) for a more detailed description of lag analysis. First-order linear regression was used except in cases where scatter plots suggested nonlinear or second-order equations were appropriate. Table curve 2.0 was used for final fit analyses. Regressions were conducted using either (1) all data from 2001 and 2002, (2) data from 2001 only, (3) data from 2002 only, (4) data from drought months only (defined as the rain-free period), or data from the nondrought months only (defined as the period within which rain events occurred). In some cases an iterative regression procedure was also utilized. The chance for testing a false positive through repeated regression analysis exists, therefore we argue that these results should serve as future hypotheses, not conclusive, causal results. To test the hypothesis that $\delta^{13}C_R$ was different between the two forests a *t*-test assuming unequal variance was used because the homogeneity of variance

Table 1 General $\delta^{13}C_R$ statistics for the ponderosa pine and Douglas-fir forests

	ponderosa pine	Douglas-fir
Mean $\delta^{13}C_R$	−25.41	−26.23
Standard deviation	1.67	1.82
Standard error	0.23	0.28
Total sample size*	51	42
Maximum $\delta^{13}C_R$	−21.20	−21.15
Minimum $\delta^{13}C_R$	−30.02	−29.71
Total range	−8.83	−8.56

All values are in ‰.

*Defined as the total number of Keeling plots used in analyses.

Table 2 Summary of correlation analyses for $\delta^{13}C_R$ vs. meteorological and physiological variables at the Douglas-fir site during 2002

(x)	Lag	Average	r^2	P	a	b	Form	Day of year (year)	n
PAR	5	0	0.10	0.090	−27.65	0.055	$\delta^{13}C_R = a + bx$	53–298 (2002)	33
SWC	0	1	0.22	**0.007**	−24.02	−7.10	$\delta^{13}C_R = a + bx$	53–298 (2002)	33
SWC[*]	0	1	0.65	**<0.001**	−23.30	−9.91	$\delta^{13}C_R = a + bx$	53–255 (2002)	30
SWC[†]	0	1	0.68	**<0.001**	−29.59	−2.56	$\delta^{13}C_R = a + b \ln x$	53–255 (2002)	30
T_{air}	0	1	0.11	0.076	−27.52	0.13	$\delta^{13}C_R = a + bx$	53–298 (2002)	33
T_{soil}	0	1	0.16	**0.025**	−27.02	0.001	$\delta^{13}C_R = a + bx^3$	53–298 (2002)	33
T_{soil}[‡]	0	1	0.45	**0.006**	−34.50	0.733	$\delta^{13}C_R = a + bx$	162–255 (2002)	15
Precipitation[§]	0	1	0.17	**0.018**	−26.97	−0.026	$\delta^{13}C_R = a + b \ln x$	53–298 (2002)	33
Precipitation[¶]	0	10	0.17	**0.020**	−25.14	−0.423	$\delta^{13}C_R = a + bx^{0.5}$	53–298 (2002)	33
vpd	0	1	0.20	**0.008**	−27.10	1.461	$\delta^{13}C_R = a + bx$	53–298 (2002)	33
vpd[**]	3	1	0.48	**<0.001**	−27.75	2.048	$\delta^{13}C_R = a + bx$	53–255 (2002)	30
vpd[††]	0	5	0.46	**<0.001**	−27.96	2.285	$\delta^{13}C_R = a + bx$	53–255 (2002)	30
Cumulative *vpd*[‡‡]		Variable	0.17	**0.019**	−26.18	0.461	$\delta^{13}C_R = a + b \ln x$	53–298 (2002)	33
Cumulative *vpd*[§§]		Variable	0.19	**0.012**	−26.35	0.389	$\delta^{13}C_R = a + b \ln x$	53–298 (2002)	33
Cumulative *vpd*[¶¶]		Variable	0.41	**<0.001**	−27.43	0.757	$\delta^{13}C_R = a + bx^{0.5}$	53–255 (2002)	30

The form of the equation is indicated under the column labeled Form. Details on the regression analyses can be found in the Methods. To save space, only the regression from the time period that provided the best statistical fit is presented, or if no relationship was significant, the results from regression of all Keeling plot data collected in 2002 are shown. The number of days lagged, the number of days averaged, the coefficient of determination (r^2), the P-value of the regression, and the coefficients (a, b) are presented. Significant P-values ($\alpha \leq 0.05$) are given in bold. A zero-day lag with a 1-day average (0, 1) is identical to saying that yesterday's weather was regressed against last night's isotopic signature. See text for further details on the regression analyses.

[*] $\delta^{13}C_R$ vs. *SWC* with three postdrought outliers removed, linear equation for comparison to *SWC* with no outliers removed.

[†] $\delta^{13}C_R$ vs. *SWC* with three postdrought outliers removed, best-fit equation.

[‡] $\delta^{13}C_R$ vs. soil temperature during period of no precipitation, summer 2002.

[§] $\delta^{13}C_R$ vs. daily precipitation.

[¶] $\delta^{13}C_R$ vs. 10 days cumulative precipitation.

[**] $\delta^{13}C_R$ vs. *vpd* with three postdrought outliers removed.

[††] $\delta^{13}C_R$ vs. 5-day average *vpd*.

[‡‡] $\delta^{13}C_R$ vs. cumulative *vpd* after the last previous precipitation event.

[§§] $\delta^{13}C_R$ vs. cumulative *vpd* after the last previous precipitation event, where rain events are defined as ≥ 0.2 cm.

[¶¶] $\delta^{13}C_R$ vs. cumulative *vpd* after the last previous precipitation event with three postdrought outliers removed.

PAR, Photosynthetically active radiation; *SWC*, soil water content; *vpd*, vapor pressure deficit.

assumption was not met, precluding the use of repeated measures analysis of variance. SYSTAT 10.0 was used for statistical analyses.

Although we did extensive statistical tests to investigate time lags (>13 000 lag-analysis regressions were performed), we did not allocate extensive text towards the question of time lags beyond ascertaining the time lags with the highest fit statistics for purpose of identifying $\delta^{13}C_R$–climate relationships (time lags are presented in Tables 2–4). The reason for this is because the time it takes for a carbon atom to move from foliage to the site of respiration is unlikely to be constant, but rather, it probably shifts with changes in carbon allocation, tissue metabolism, temperature, etc. We were unable to detect within-site variability in lag times despite our relatively large sampling frequency. Detailed lag analysis will require a higher frequency data set than we had in the current study.

Results

Meteorological patterns

Figure 2a–f shows the climatic patterns during the sampling period. Precipitation is unimodal at both sites, with pronounced dry periods in the summer and substantial precipitation in the autumn, winter and spring. *vpd* and T_{air} exhibited maximum values during the drought period. As expected from their different proximity to the Pacific Ocean, the Douglas-fir site typically had lower *vpd*, smaller diel and seasonal ranges of T_{air} and more precipitation than the ponderosa pine site. The Douglas-fir site experienced 155 consecutive days with the minimum daily (24 h) air temperature (T_{min}) greater than 0.2 °C (the $\delta^{13}C_R$ freeze cutoff identified in Bowling *et al.*, 2002). The ponderosa pine forest had 76 consecutive days above 0.2 °C, half as many as the Douglas-fir forest.

Table 3 Summary of correlation analyses for $\delta^{13}C_R$ vs. meteorological and physiological variables at the ponderosa pine site, 2001 and 2002

(x)	Lag	Average	r^2	P	a	b	Form	Day of year (year)	n
G_c	2	2	0.36	**0.001**	−27.74	−2.74	$\delta^{13}C_R = a + b\ln(x/x)$	120–312 (2001) & 119–298 (2002)	39
PAR	2	1	0.32	0.069	−26.38	0.03	$\delta^{13}C_R = a + bx$	169–242 (2002)	11
SWC	2	1	0.01	0.41	−25.62	−0.01	$\delta^{13}C_R = a + b\ln(x/x^2)$	120 (2001) through 298 (2002)	51
T_{air}	0	1	0.10	**0.024**	−26.21	0.076	$\delta^{13}C_R = a + bx$	120 (2001) through 298 (2002)	51
T_{soil}[*]	0	1	0.08	**0.047**	−25.77	0.001	$\delta^{13}C_R = a + bx^3$	120 (2001) through 298 (2002)	51
T_{soil}[†]	0	1	0.07	0.067	−25.81	0.003	$\delta^{13}C_R = a + bx^2$	120 (2001) through 298 (2002)	51
T_{soil}[‡]	0	1	0.58	**0.001**	−28.12	0.216	$\delta^{13}C_R = a + bx$	150–255 (2002)	17
Precipitation[§]	0	1	0.07	0.066	−25.46	0.002	$\delta^{13}C_R = a + be^{x}$	120 (2001) through 298 (2002)	51
Precipitation[¶]	0	10	0.01	0.377	−25.56	0.481	$\delta^{13}C_R = a + be^{-x}$	120 (2001) through 298 (2002)	51
vpd	0	1	0.11	**0.020**	−26.02	0.742	$\delta^{13}C_R = a + bx$	120 (2001) through 298 (2002)	51
vpd[**]		Variable	0.02	0.295	−25.59	0.041	$\delta^{13}C_R = a + bx$	120 (2001) through 298 (2002)	51

Regression analyses, data organization and table presentation are similar to that done for the Douglas-fir data set (see caption for Table 2). See caption for Table 2 and the Methods text for further details on the regression analyses.

[*] $\delta^{13}C_R$ vs. soil temperature measured at 15 cm depth.

[†] $\delta^{13}C_R$ vs. soil temperature measured at 2 cm depth.

[‡] $\delta^{13}C_R$ vs. soil temperature measured at 15 cm depth, using only data from the rain-free period in 2002.

[§] $\delta^{13}C_R$ vs. daily precipitation.

[¶] $\delta^{13}C_R$ vs. 10 days cumulative precipitation.

[**] $\delta^{13}C_R$ vs. cumulative *vpd* since the last precipitation event.

PAR, Photosynthetically active radiation; *SWC*, soil water content; *vpd*, vapor pressure deficit.

Table 4 Summary of correlation analyses for $\delta^{13}C_R$ vs. meteorological and physiological variables for both sites combined (Douglas-fir and ponderosa pine)

(x)	+/−	r^2	P	a	b	Form	Day of year (year)	n
PAR	+	0.09	**0.009**	−26.89	0.038	$\delta^{13}C_R = a + bx$	120 (2001)–298 (2002)	84
SWC	−	0.13	**0.001**	−24.58	−5.57	$\delta^{13}C_R = a + bx$	120 (2001)–298 (2002)	84
SWC[*]	−	0.51	**<0.001**	−28.95	−1.91	$\delta^{13}C_R = a + b\ln x$	120 (2001)–298 (2002)	84
T_{air}	+	0.12	**0.002**	−26.75	0.097	$\delta^{13}C_R = a + bx$	120 (2001)–298 (2002)	84
T_{soil}[†]	+	0.11	**0.003**	−26.15	0.001	$\delta^{13}C_R = a + bx^3$	120 (2001)–298 (2002)	84
T_{soil}[‡]	+	0.39	**<0.001**	−14.45	−27.76	$\delta^{13}C_R = a + bx^3$	150–255 (2002)	32
Precipitation[§]	−	0.07	**0.017**	−26.91	1.463	$\delta^{13}C_R = a + be^{-x}$	120 (2001)–298 (2002)	84
Precipitation[¶]	−	0.08	**0.013**	−25.14	−0.269	$\delta^{13}C_R = a + bx^{0.5}$	120 (2001)–298 (2002)	84
vpd	+	0.18	**<0.001**	−26.56	1.053	$\delta^{13}C_R = a + bx$	120 (2001)–298 (2002)	84
vpd[**]	+	0.26	**<0.001**	−26.80	1.253	$\delta^{13}C_R = a + bx$	120 (2001)–298 (2002)	84
Cumulative *vpd*[††]	+	0.10	**0.005**	−25.86	0.329	$\delta^{13}C_R = a + b\ln x$	120 (2001)–298 (2002)	84
Cumulative *vpd*[‡‡]	+	0.13	**0.001**	−25.92	0.354	$\delta^{13}C_R = a + b\ln x$	120 (2001)–298 (2002)	84

Regression analyses, data organization and table presentation are similar to that done for the ponderosa pine and Douglas-fir data sets (see captions for Tables 2 and 3). The lag and averaging periods are the same as presented in Tables 2 and 3 for ponderosa pine and Douglas-fir, respectively, and are not presented in this table. See captions for Tables 2 and 3 and the Methods text for further details on the regression analyses.

[*] $\delta^{13}C_R$ vs. *SWC* with three postdrought outliers removed from the Douglas-fir data set.

[†] $\delta^{13}C_R$ vs. soil temperature using 15 and 10 cm measurement depths for the pine and Douglas-fir forests, respectively.

[‡] $\delta^{13}C_R$ vs. soil temperature during the rain free periods in 2002.

[§] $\delta^{13}C_R$ vs. daily precipitation.

[¶] $\delta^{13}C_R$ vs. cumulative precipitation.

[**] $\delta^{13}C_R$ vs. *vpd* with three postdrought outliers removed from the Douglas-fir data set.

[††] $\delta^{13}C_R$ vs. cumulative *vpd*.

[‡‡] $\delta^{13}C_R$ vs. cumulative *vpd* with three postdrought outliers removed from the Douglas-fir data set.

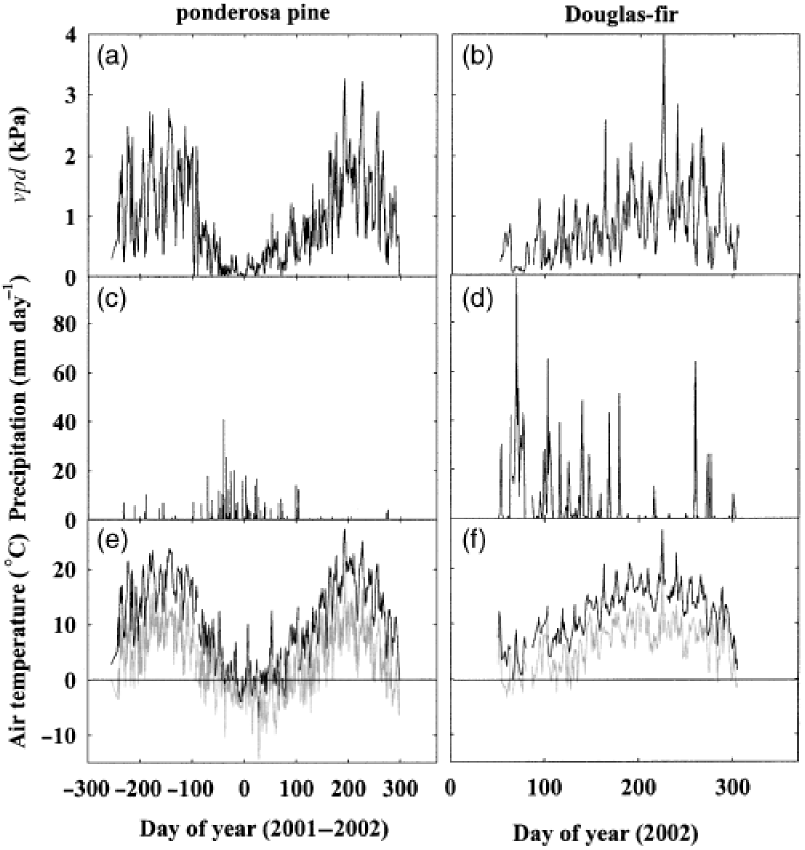

Fig. 2 Meteorological conditions at the ponderosa pine (left-hand figures) and Douglas-fir (right-hand figures) forests. The ponderosa pine forest was monitored in 2001 and 2002, so the *x*-axis is portrayed as the day of year relative to day 1, 2002. The Douglas-fir forest was only measured in 2002 and the *x*-axis is scaled appropriately. (a, b) Daylight mean *vpd*, (c, d) daily precipitation and (e, f) daily mean (black line) and minimum (gray line) air temperature.

Seasonal variation in $\delta^{13}C_R$

Figure 3 shows the seasonal course for $\delta^{13}C_R$ and *SWC* at the Douglas-fir forest, and descriptive statistics are provided in Table 1. The pronounced summer drought is visible in *SWC* between days 190 and 260, and with the exception of a few small rain events between days 260 and 300, the drought continued much longer into the autumn than is typical of this area (Taylor & Hannan, 1999). Observed $\delta^{13}C_R$ ranged from −21.2‰ to −29.7‰ (range of 8.6‰) and was generally more negative when *SWC* was high and more positive as *SWC* decreased. The noticeable $\delta^{13}C_R$ enrichment from the winter minimum on day 100 to the summer maximum on day 250 was ~ 5.1‰.

Figure 4 shows the seasonal course for $\delta^{13}C_R$, *SWC* and Ψ_s calculated from predawn leaf water potential at the ponderosa pine forest. Descriptive statistics are provided in Table 1. The summer drought is readily visible in *SWC* between days 180 and 300. Observed $\delta^{13}C_R$ ranged from −21.2‰ to −30.0‰ (range of 8.8‰) and was generally more negative when *SWC* was high and more positive as *SWC* decreased. Observed $\delta^{13}C_R$ more closely followed Ψ_s in 2001 than 2002, but was not significantly related over the entire study period ($r^2 = 0.18$, $P = 0.20$). The pine site exhibited a much smaller winter-to-summer $\delta^{13}C_R$ enrichment than the Douglas-fir forest; with a $\delta^{13}C_R$ increase of ~ 2.0‰.

Hypotheses tests

It is well established that $\delta^{13}C_R$ is typically more enriched at ecosystems that receive low amounts of precipitation compared with high rainfall ecosystems (Bowling *et al.*, 2002; Pataki *et al.*, 2003). This pattern was supported in our study, in which mean annual $\delta^{13}C_R$ was −25.41‰ (SE, 0.23) for the ponderosa pine forest and −26.23‰ (SE, 0.28) for the Douglas-fir forest (Table 1, $P = 0.07$).

Summaries of the regression analyses are shown for the Douglas-fir forest in Table 2, the ponderosa pine

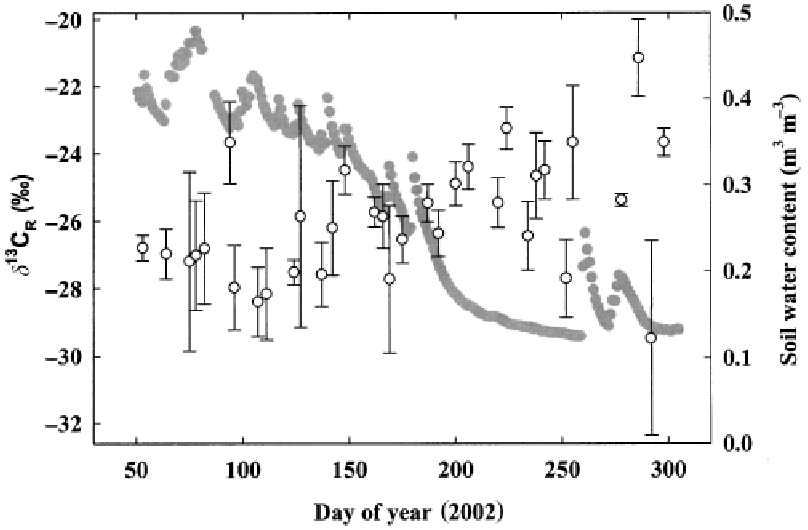

Fig. 3 $\delta^{13}C_R$ (open symbols) and soil water content (*SWC*, gray symbols) measured at the Douglas-fir forest vs. day of year, 2002. Bars are standard errors.

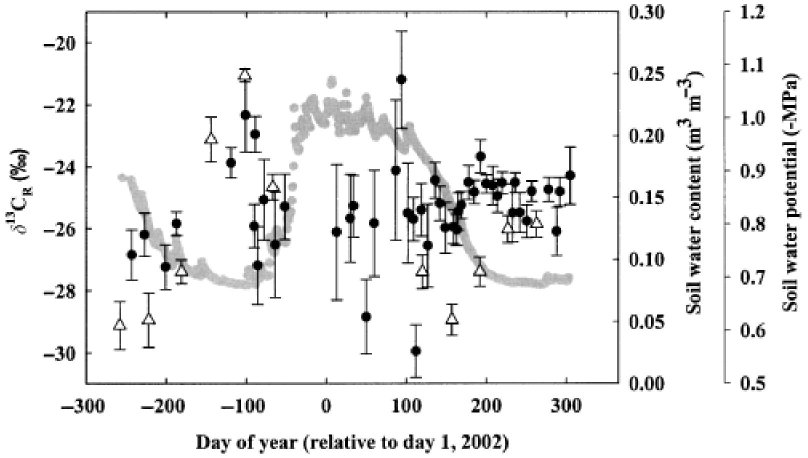

Fig. 4 $\delta^{13}C_R$ (black symbols) and soil water content (*SWC*) (gray symbols) measured at the ponderosa pine forest vs. day of year relative to day 1, 2002. Also shown is soil water potential (−MPa) derived from predawn water potentials on old-growth pine trees (open triangles). Bars are standard errors.

forest in Table 3 and both sites combined in Table 4. Only the regression with the best fit is provided for each $\delta^{13}C_R$ vs. parameter correlation. The lag times are also provided in each table.

The direct test of the hypothesis that freezing T_{min} ($<0.2\,^{\circ}C$) are associated with enriched values of $\delta^{13}C_R$ is shown in Figs 5a and b. Neither the Douglas-fir nor the ponderosa pine site exhibited a consistent enrichment when T_{air} dropped below $<0.2\,^{\circ}C$, and the SE in $\delta^{13}C_R$ was substantial for the subfreezing temperatures, particularly in the pine forest. For this analysis, the minimum air temperature in the last 5 days was used; however, using T_{min} from 1, 3 or 10 days ago gave similar results (data not shown).

The relationships between $\delta^{13}C_R$ and *SWC* for the Douglas-fir and ponderosa pine forests are shown in Fig. 6. Mean monthly values are presented to highlight the long-term trend (Lai *et al.*, 2004). For the Douglas-fir forest a significant negative relationship was observed ($r^2 = 0.83$, $P < 0.001$), however, the ponderosa pine forest exhibited no significant relationship.

The direct test of the hypothesis that increasing *vpd* is associated with enriched values of $\delta^{13}C_R$ is shown in Figs 7a and c, and G_c for the ponderosa pine site is shown in (Fig. 7b). The hypothesis was not supported at the ponderosa pine site as no relationship was observed for $\delta^{13}C_R$ vs. *vpd* regardless of lag time (Table 3, Fig. 7a). The open triangles in Fig. 7a

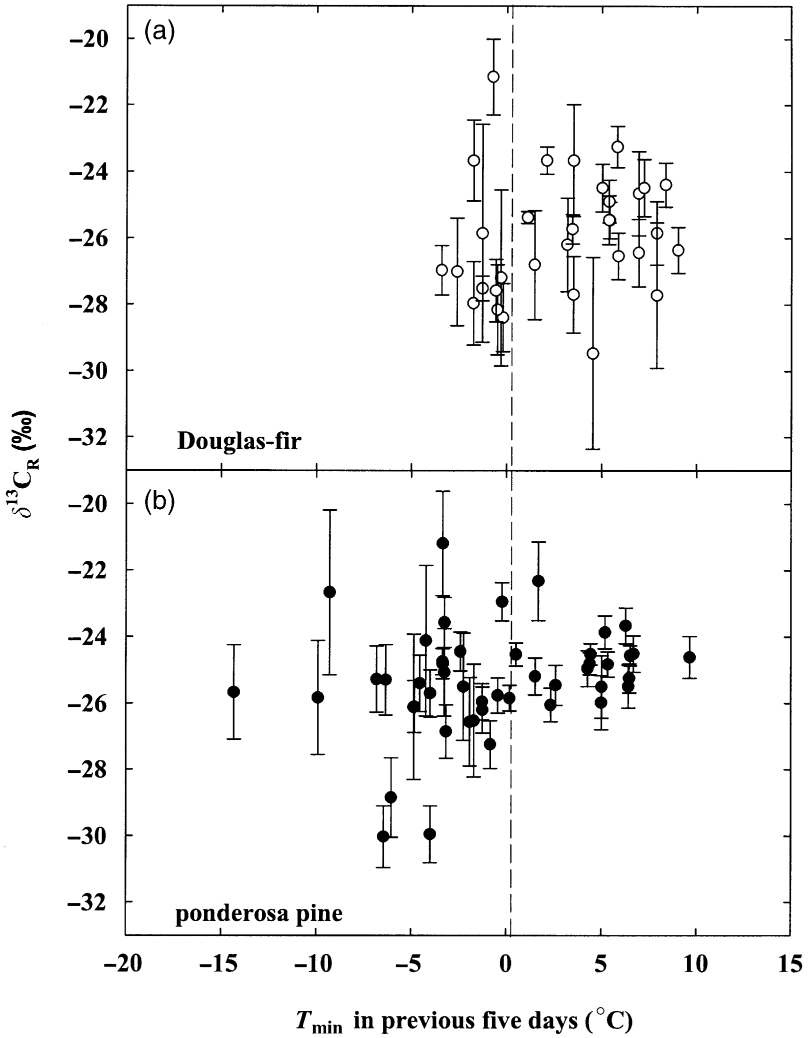

Fig. 5 (a) $\delta^{13}C_R$ vs. T_{min} at the Douglas-fir forest. (b) $\delta^{13}C_R$ vs. T_{min} at the ponderosa pine forest. T_{min} is defined within this analysis as the minimum air temperature within the last 5 consecutive days prior to sampling. Bars are standard errors.

represent the data published in Bowling *et al.* (2002). G_c increased with *vpd* from 0.0 to 0.75 kPa, then declined with increasing $vpd > 0.75$ kPa (Fig. 7b). The hypothesis was supported at the Douglas-fir forest, however, as $\delta^{13}C_R$ exhibited a significant increase with increasing *vpd* (Fig. 7c). When 30-day average $\delta^{13}C_R$ was compared with 30-day average *vpd* to highlight the long-term trend (similar to Fig. 6) the relationship was very strong ($r^2 = 0.85$, $P < 0.001$, Fig. 7c).

We investigated relationships between $\delta^{13}C_R$ and soil temperature because of the well-known correlation between soil temperature and the rate of respiration and because soil respired $\delta^{13}C$ should play a substantial role in $\delta^{13}C_R$ (Mortazavi & Chanton, 2002; McDowell *et al.*, 2004). Relatively poor relationships were observed for both sites when all data from throughout the year were correlated (Tables 2 and 3). However, a significant increase in $\delta^{13}C_R$ was observed with increasing soil temperature during the rain-free period at both sites (Figs 8a and b). The rain-free period is defined simply as the period during which little or no rain fell (< 3 mm day^{-1}), and lasts from days 162 to 252 at the Douglas-fir forest and days 150–255 at the ponderosa pine forest.

Figure 9 shows the direct test of the hypothesis that G_c affects $\delta^{13}C_R$. $\delta^{13}C_R$ exhibited a significant but moderately weak decline with increasing G_c ($r^2 = 0.36$, $P < 0.001$). The decline was consistent with the prediction based on leaf-level understanding of Δ and G_c (Fig. 1b).

Discussion

Our *a priori* prediction was that variation in $\delta^{13}C_R$ associated with site and season would be consistent

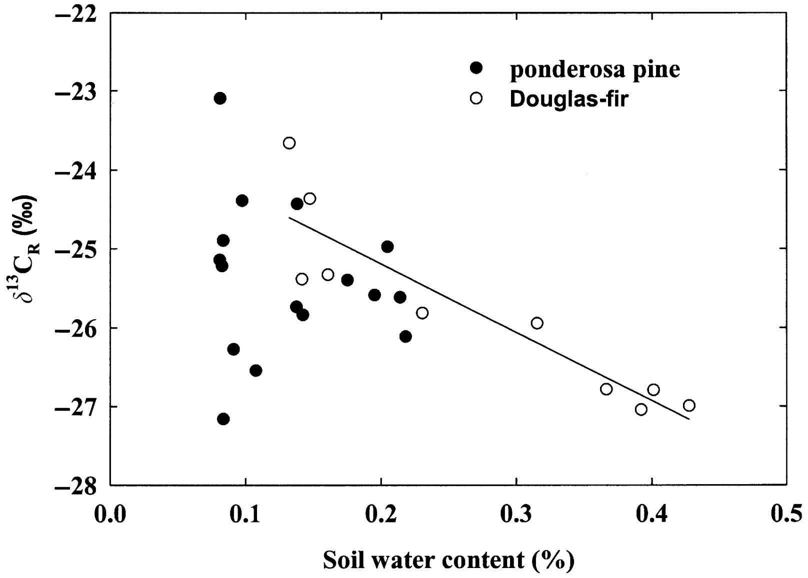

Fig. 6 Mean monthly (30 days) $\delta^{13}C_R$ vs. mean monthly soil water content (*SWC*) at the Douglas-fir (open symbols) and ponderosa pine (filled symbols) forests. The regression is for the Douglas-fir forest alone: $\delta^{13}C_R = -8.7(SWC) - 23.5$, $r^2 = 0.83$, $P < 0.01$. No significant regression was observed at the ponderosa pine forest. Note that the *SWC* sensors were not cross-calibrated between sites and therefore *SWC* should not be compared between sites. Error bars are omitted for clarity, but averaged 1.44‰ and 1.54‰, respectively, for the ponderosa pine and Douglas-fir sites.

with stomatal control over Δ (Fig. 1). Although the results were not as simple or clear as those presented by Bowling *et al.* (2002), they are consistent with our overall hypothesis. Similar to our previous finding, respired CO_2 from the drier ponderosa pine forest was consistently more enriched than the wetter Douglas-fir forest (Table 1). Both sites exhibited drought-related enrichment of $\delta^{13}C_R$ (Figs 3 and 4), although the enrichment at the Douglas-fir forest was more than twice that of the pine forest. The Douglas-fir forest was particularly sensitive to climatic variation (e.g. *SWC*, *vpd*) in a manner consistent with stomatal control over Δ (Figs 3, 6 and 7). Finally, the ponderosa pine forest exhibited the predicted relationship between $\delta^{13}C_R$ and G_c (Figs 1b and 9), albeit weakly. However, we also observed $\delta^{13}C_R$ variability that remains unexplained, as well as highly significant relationships that were not predicted *a priori*. Notable among these are the strong $\delta^{13}C_R$–soil temperature relationships (Fig. 8), suggesting a significant role of belowground respiration on ecosystem-scale $\delta^{13}C_R$. To our knowledge, this is the first report of $\delta^{13}C_R$–soil temperature relationships.

The observation that the drier ponderosa pine forest was typically more enriched than the wetter Douglas-fir forest (Table 1) was not surprising because many studies have shown that organic $\delta^{13}C$ as well as respired $\delta^{13}C$ are typically enriched in drier climates (Schulze *et al.*, 1998; Bowling *et al.*, 2002; Pataki *et al.*, 2003). There are many factors that could enrich $\delta^{13}C_R$ at the ponderosa pine forest relative to the Douglas-fir forest. Foliar $\delta^{13}C$ of ponderosa pine was slightly enriched above that of Douglas-fir (var. *glauca*) in a common garden study suggesting that ponderosa pine are intrinsically (genetically) predisposed to lower Δ and enriched $\delta^{13}C$ (Marshall *et al.*, 2001). Additionally, hydraulic limitations of G_c associated with tree height and subsequent decline in Δ is well established (Yoder *et al.*, 1994; Hubbard *et al.*, 1999; McDowell *et al.*, 2002). Therefore, it is likely that the relatively tall ponderosa pine trees (~ 33 m for the overstory trees) experience lower Δ than the relatively shorter Douglas-fir trees (~ 9 m for the Douglas-fir plantation) further enriching $\delta^{13}C$ of photosynthate at the ponderosa pine forest compared with the Douglas-fir forest.

A more surprising result was that the Douglas-fir forest, which experiences a mild climate because of the close proximity of the Pacific Ocean (typical of a coastal environment), exhibited more than twice the enrichment from winter to summer than the ponderosa pine forest, which experiences much larger climatic swings (typical of a continental climate). This can be seen by comparison of the $\delta^{13}C_R$ enrichment from ~days 100 to 200, 2002, in Figs 3 and 4, in which $\delta^{13}C_R$ of the Douglas-fir forest increases by ~5‰ compared with the ~2‰ increase at the ponderosa pine forest. Ometto *et al.* (2002) observed in a comparison of two sites in the

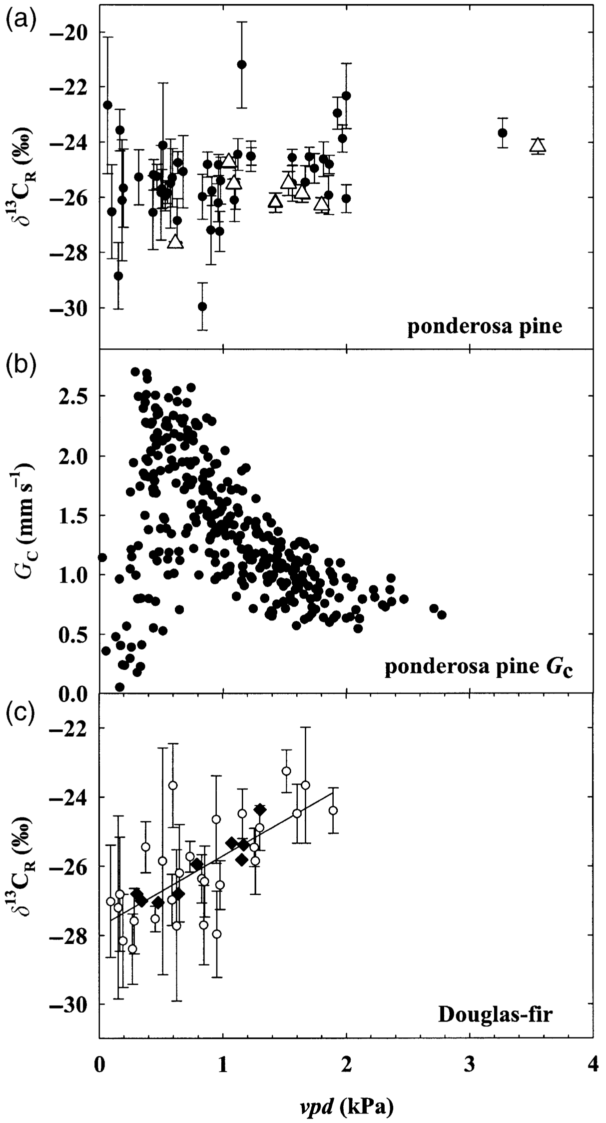

Fig. 7 (a) $\delta^{13}C_R$ vs. vapor pressure deficit (*vpd*) at the ponderosa pine forest. $\delta^{13}C_R$ is lagged 1 day behind *vpd* (Table 3). The open triangles represent the data points for this forest published in Bowling *et al.* (2002), in which $\delta^{13}C_R$ was lagged 5 days behind *vpd*. There was no significant relationship observed for data collected by the autosampler. (b) G_c vs. *vpd* at the ponderosa pine forest. G_c data is averaged for 11:00 to 13:00 hours to avoid errors associated with capacitance, and is shown against daylight average *vpd* for the individual day. The G_c data is not lagged behind *vpd*. (c) $\delta^{13}C_R$ vs. *vpd* at the Douglas-fir forest. $\delta^{13}C_R$ is lagged 3 days behind *vpd*. The open symbols represent individual nightly Keeling plot intercepts, and the filled diamonds represent monthly average values. The regression is $\delta^{13}C_R = 2.05vpd - 27.75$, $r^2 = 0.48$, $P < 0.001$, and does not include the three low-*vpd* points discussed in relation to Fig. 3 (see Discussion). The regression for the monthly average values (not shown), which includes all points is $\delta^{13}C_R = 2.25vpd - 27.85$, $r^2 = 0.85$, $P < 0.001$.

Amazon basin that seasonality in precipitation had a significant effect on the temporal dynamics of $\delta^{13}C_R$; however, in our study both sites experienced similar seasonality in precipitation, with wet winters followed by dry summers. In fact, the ponderosa pine forest experienced a substantially more protracted rain-free period than the Douglas-fir forest (Figs 2c and d), which we might expect to cause even greater enrichment. Additionally, precipitation amount proceeding isotopic sampling was not observed to be a significant factor in this study (Tables 2–4). Therefore, differences in seasonality of precipitation cannot explain the large differences in drought-related enrichment between the two forests.

A number of potential mechanisms exist to explain the site-specific differences in drought-associated $\delta^{13}C_R$ enrichment, and it is likely that multiple interacting factors are responsible. One plausible explanation resides with groundwater availability, which is suspected at the pine forest based on rooting depth, modeling, sapflow and stable isotope studies (Law *et al.*, 2001; Williams *et al.*, 2001; Brooks *et al.*, 2002; Bowling *et al.*, 2003). Our own analyses of soil and xylem water $\delta^{18}O$ collected bimonthly from the Douglas-fir and pine forests support the contention that the pine forest has access to groundwater throughout 2002, while the Douglas-fir forest relied on surface water that is subject to drought (Fig. 10). We sampled xylem water via increment cores and soil water from the upper 10 cm of the mineral soil. At the pine site we also sampled water from a nearby spring located ~ 1 km and slightly downhill from our sampling location (there was no nearby spring at the Douglas-fir forest). More details on laboratory methods and $\delta^{18}O$ data from years prior to 2002 can be found in Bowling *et al.* (2003). Xylem water of pine trees was ~ 100% derived from groundwater during the majority of 2002 except during peak drought (days 200–270) when groundwater still provided an average of 76% of pine xylem water (range 70–84%). Estimates of drought-period groundwater use are conservative because hydraulic redistribution of groundwater to the upper soil contributes ~ 35% of daily water utilization during drought (Brooks *et al.*, 2002). In contrast, Douglas-fir xylem water showed much smaller deviation from soil water $\delta^{18}O$ suggesting that those trees do not have much, if any, groundwater access (although they do exhibit a small shift during drought that may be associated with drawing water from deeper level in the soil profile than we sampled). These mixing curve analyses assume that there are only two sources of water, the upper 10 cm and groundwater, an assumption that is likely false. However, the general conclusion is likely to hold even if trees from either stand access

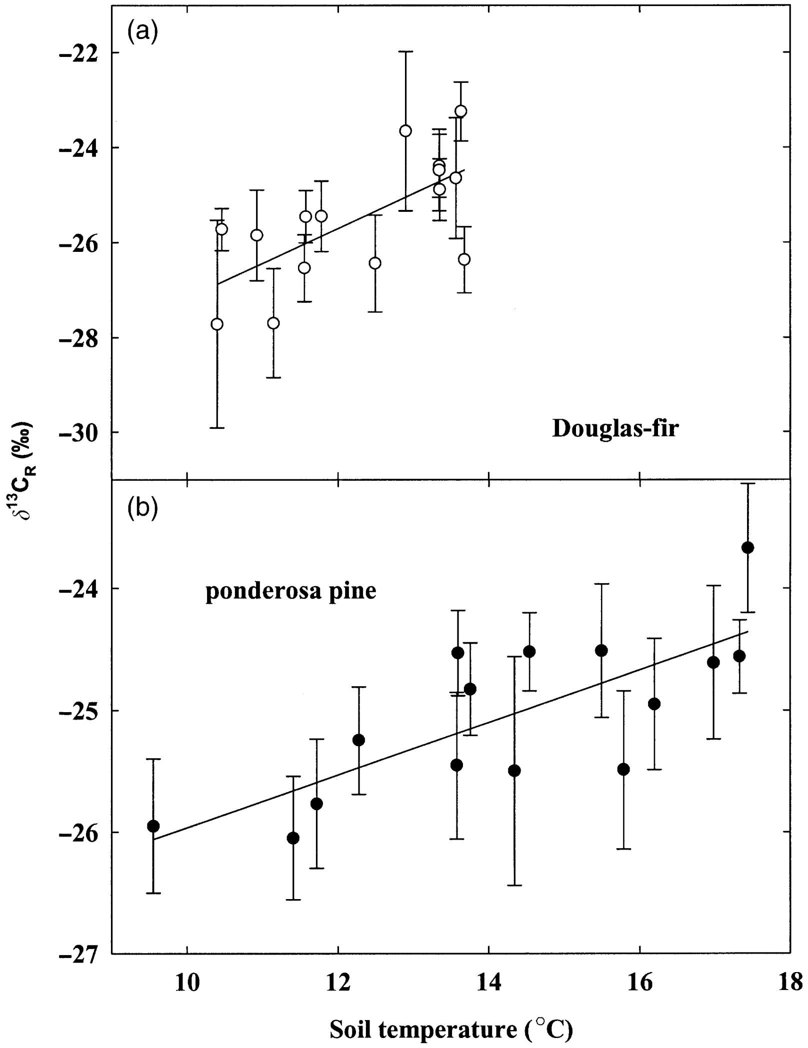

Fig. 8 (a) $\delta^{13}C_R$ of the Douglas-fir forest vs. soil temperature measured at 10 cm depth, for the rain-free period (days 162–252, 2002). Soil temperature is the 24 h average including the night that flask collection was initiated for a given Keeling plot. The regression is $\delta^{13}C_R = 0.73T_{soil}-34.5$, $r^2 = 0.45$, $P < 0.01$. (b) $\delta^{13}C_R$ of the ponderosa pine forest vs. soil temperature measured at 15 cm depth, for the rain-free period (days 150–255, 2002). Soil temperature is the 24 h average including the night that flask collection was initiated for a given Keeling plot. The regression is $\delta^{13}C_R = 0.22T_{soil}-28.1$, $r^2 = 0.58$, $P < 0.01$.

water from below 10 cm but above the water table. Therefore, it appears that the pine forest has groundwater access.

At the ponderosa pine forest, the relatively minimal enrichment during drought (Fig. 4) and the lack of relationships between $\delta^{13}C_R$ and *SWC* (Fig. 6) and *vpd* (Fig. 7a) may result from groundwater buffering $\delta^{13}C_R$ from climate. Groundwater access would relegate *SWC* in the upper soil horizons to a less important role in regard to canopy physiology (although it may remain critical for root and heterotrophic metabolism), and likewise, a lack of water limitation will act to buffer Δ from *vpd*. Notably, the data from our previous research at the ponderosa pine forest (Bowling *et al.*, 2002) shown in Fig. 7a falls in line with our current data set. In that previous study we proposed that a $\delta^{13}C_R$–*vpd* relationship was apparent when all sites were considered together. In the current study, $\delta^{13}C_R$ of the Douglas-fir forest was sensitive to both *SWC* (Fig. 6) and *vpd* (Fig. 7c). A similar $\delta^{13}C_R$–*SWC* pattern has been shown for an old-growth Douglas-fir forest in Washington State that has little or no groundwater access during drought (Fessenden & Ehleringer, 2003, T. Link, personal communication). Given the lack of a *vpd*–$\delta^{13}C_R$ relationship at the ponderosa pine forest, we suggest that $\delta^{13}C_R$–climate relationships may be mitigated by groundwater access.

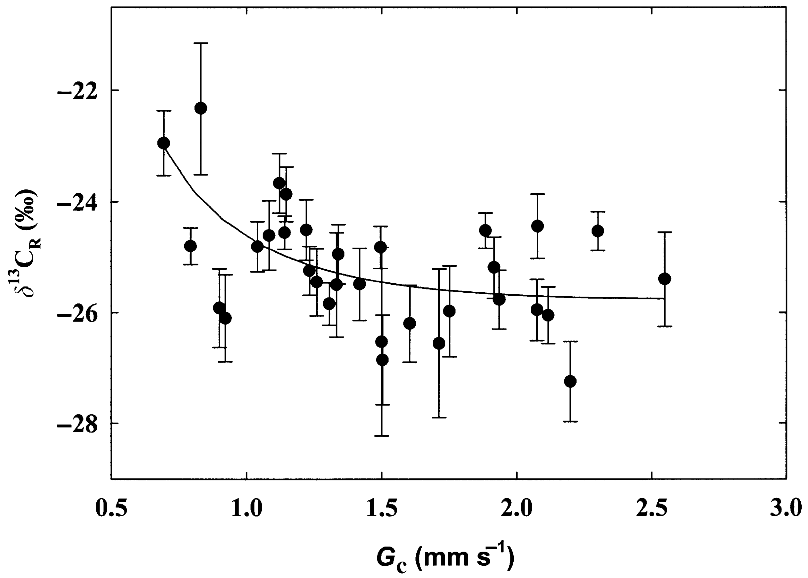

Fig. 9 $\delta^{13}C_R$ of the ponderosa pine forest vs. G_c. Sapflow was not measured during the winter months, limiting our sample size to 39 periods during which both sapflow and corresponding $\delta^{13}C_R$ data were available (120–312, 2001, and 119–298, 2002). The G_c data is averaged from 11:00 to 13:00 hours to avoid errors associated with capacitance. The figure utilizes G_c data from 2 days prior to flask collection, and is averaged for 2 days (i.e. if flasks were collected on day 100, G_c data is averaged for days 98 and 99). This was the lag and averaging period that provided the best fit. The best-fit equation, provided for reference, is $\delta^{13}C_R = -24.62–3.07 \ln (G_c/G_c)$, $r^2 = 0.36$, $P < 0.001$.

Despite groundwater access buffering the ponderosa pine forest from climate, we still observed a significant (but weak) relationship between $\delta^{13}C_R$ and G_c that was consistent with our prediction (Figs 1b and 9). We reran the regression without data below 0.9 mm day^{-1} because of concern that the few low G_c points were forcing the relationship, but the regression remained significant ($\delta^{13}C_R = -24.11–4.89 \ln (G_c/G_c)$, $r^2 = 0.25$, $P = 0.009$). During periods of high G_c (>1.9 mm day^{-1}) it is likely that other, nonstomatal factors regulate Δ (such as *PAR* or air temperature) and $\delta^{13}C_R$ (such as soil temperature). The fact that this relationship was significant and consistent with our prediction, despite groundwater buffering, lends support to the idea that there is a stomatal component to $\delta^{13}C_R$ regulation.

At the Douglas-fir forest, where we had no sapflow data, we relied on more traditional $\delta^{13}C_R$–climate relationships to gain insight on the factors and mechanisms that may control $\delta^{13}C_R$. To assess the role of stomata, we hypothesized that declining *SWC* and increasing *vpd* should both be associated with enriched $\delta^{13}C_R$ because of reductions in G_c and subsequent reductions in Δ *if* leaf-level Δ is propagated to the ecosystem scale. The $\delta^{13}C_R$–*SWC* relationship observed at the Douglas-fir forest (Fig. 6) is consistent with this hypothesis. Notably, deviations from the $\delta^{13}C_R$ enrichment over time shown in Fig. 3 were also consistent with leaf-level regulation of Δ, although not due solely to stomatal regulation. For example, the two enriched $\delta^{13}C_R$ values before day 150 (−23.66‰ and −24.48‰) were the first periods of high *PAR* (37–45 mol day^{-1}) in the spring after months of low *PAR* (<20 mol day^{-1}). This is consistent with high *PAR* causing elevated photosynthetic rates, a subsequent decline in c_i/c_a, and decreased Δ (Zimmerman & Ehleringer, 1990). Similarly, the first periods of low *PAR* in the autumn after many months of relatively high *PAR* were associated with depleted $\delta^{13}C_R$ values (these are the depleted $\delta^{13}C_R$ values after day 220 in Fig. 3). We should note that these three low *PAR* points were also periods of low *vpd*, which should have a similar effect on Δ as increased stomatal conductance. Regressions both with and without these three points are presented in Tables 2 and 4. The $\delta^{13}C_R$–*vpd* relationship shown in Fig. 7c also supports a stomatal control over $\delta^{13}C_R$ similar to that proposed in Fig. 1a. In particular, the 30-day averages highlight that the long-term trend is for a very strong relationships between *vpd* and $\delta^{13}C_R$. Therefore, the Douglas-fir results support the notion that canopy physiology is a primary driver behind $\delta^{13}C_R$ in this forest.

Another factor that could alter Δ and hence $\delta^{13}C_R$ is seasonal changes in photosynthetic capacity (Wilson *et al.*, 2001), however, retrospective analysis of $\delta^{13}C_R$ vs. photosynthetic capacity parameters derived from A–C_i curves at the pine site (Law *et al.*, 2003) showed no correlation (best $r^2 = 0.03$). Interpretation of this

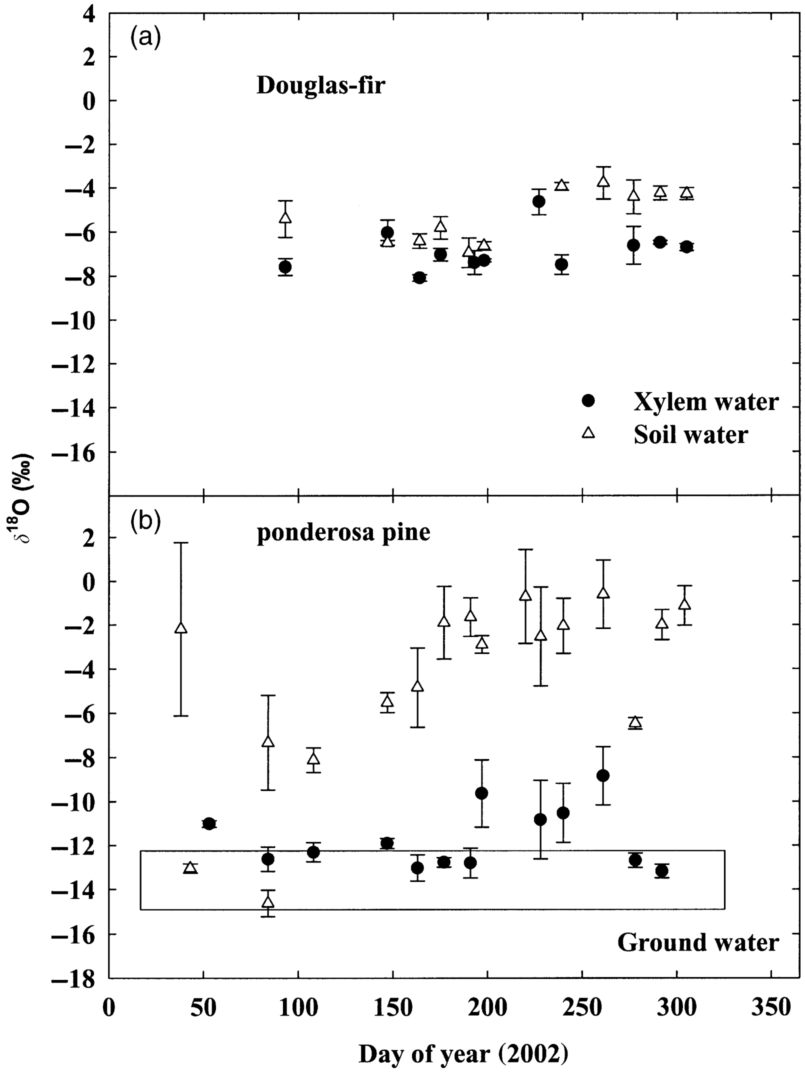

Fig. 10 (a) δ^{18}O of water extracted from xylem tissue (filled symbols) and from the upper 10 cm of the mineral soil (open triangles) at the Douglas-fir forest. Bars are standard errors of triplicate samples. (b) δ^{18}O of water extracted from xylem tissue (filled symbols) and from the upper 10 cm of the mineral soil (open triangles) at the ponderosa pine forest. The xylem δ^{18}O values are averages of the two primary age classes of trees at the site, 250- and 50-year-old trees. Bars are standard errors of triplicate samples. The rectangular box is the observed range of values for groundwater δ^{18}O collected at a nearby spring (12.5–14.7‰, from Bowling *et al.*, 2003).

analysis is constrained by the small sample size ($n = 5$) therefore firm conclusions cannot be drawn.

One initial hypothesis that was clearly rejected was the expectation that freezing air temperatures would cause a reduction in G_c and subsequent enrichment in $\delta^{13}C_R$ (Figs 1a and 5). The proposed mechanism of a freeze-induced enrichment was that freezes typically induce stomatal closure in conifers (Kaufmann, 1976; Smith *et al.*, 1984; Strand *et al.*, 2002), which should reduce Δ and subsequently enrich $\delta^{13}C_R$. However, at the ponderosa pine forest there is no relationship between freezing air temperatures and G_c during the summer (McDowell *et al.*, 2004) or analyzed for the complete year (this study, data not shown). This does not discount the hypothesis that if G_c does decline after a freeze that Δ will decline causing an enrichment in $\delta^{13}C_R$, but that this mechanism does not occur at the ponderosa pine forest studied here. Interestingly, the Douglas-fir forest did show significant $\delta^{13}C_R$ enrichment after the first freeze of the autumn (−21.15‰ on day 286) but other freezes had no detectable effect on $\delta^{13}C_R$. It is possible that for this coastal forest, the first freeze occurred prior to cold acclimation by the foliage (Oquist & Huner, 2003) resulting in the expected G_c and Δ reductions, but that subsequent acclimation of the foliage to low temperatures mitigated a Δ response to freezes. This is consistent with results from our previous research in Oregon (Ehleringer & Cook, 1998; Bowling *et al.*, 2002), which were mostly conducted in the nonwinter months when foliage is unlikely to be acclimated to cold air temperatures and the effects of freezes on Δ are more likely. Therefore, freezes may cause enriched $\delta^{13}C_R$ in some species prior to cold acclimation; however, the importance of this mechanism on an annual basis appears to be small.

The strong $\delta^{13}C_R$–soil temperature relationships observed at both sites (Fig. 8) may result from direct effects or from covariance with soil moisture (Fig. 6). Evidence for covariation is found in the significant relationship between soil moisture and temperature during the drought-free period at the Douglas-fir site ($r^2 = 0.47$, $P = 0.001$), however, no such relationship was observed at the pine site ($r^2 = 0.11$, $P > 0.10$). Separation of temperature vs. moisture effects should be tested in the future using controlled experiments.

Direct control of temperature on $\delta^{13}C_R$ is plausible. Belowground respiration rates are strongly dependent on soil temperature for the pine site (Law *et al.*, 1999) and for Douglas-fir forests (McDowell *et al.*, 2001) and soil respiration contributes ~70% of ecosystem respiration (Law *et al.*, 1999). Furthermore, $\delta^{13}C$ of roots, soil organic matter, and ectomycorrhizal fungi are typically enriched compared with foliage (Nadelhoffer & Fry, 1988; Balesdent *et al.*, 1993; Högberg *et al.*, 1999; Ehleringer *et al.*, 2000; Bhupinderpal Singh *et al.*, 2003). Therefore, increasing respiration from these isotopically enriched belowground tissues is likely to cause a corresponding enrichment in $\delta^{13}C_R$, particularly if the proportion of total ecosystem respiration contributed from belowground increases. Interestingly, the slope of the $\delta^{13}C_R$–soil temperature relationship was three times steeper at the Douglas-fir forest than the ponderosa pine forest (0.73 vs. 0.22, respectively, Tables 2 and 3), which may indicate greater sensitivity to soil temperature at the Douglas-fir forest, which has both higher *SWC* and greater soil carbon content. Our observation that the site with greater resource availability has a steeper response to soil temperature is consistent with theory regarding the dependence of respiration and cellular metabolism on rates of supply of limiting resources (Paul & Clark, 1989; Enquist *et al.*, 2003). Pulse rain events during summer drought can also result in a substantial increase in soil respiration for several days, and incubations showed much of this response is microbial (Irvine & Law, 2002; Kelliher *et al.*, 2004); the Douglas-fir forest experienced more of these events during the measurement period, which could partly explain the higher slope. Variability in isotopic fractionation during decomposition (Fernandez *et al.*, 2003) and changes in substrate (Tcherkez *et al.*, 2003) may also play a role.

Our overall interpretation of the results of this study is that canopy-scale stomatal behavior, either measured directly at the ponderosa pine forest or inferred from $\delta^{13}C_R$–climate relationships at the Douglas-fir forest, is a fundamental regulator of $\delta^{13}C_R$. However, it appears that groundwater availability can act to buffer forests from climatic (and subsequent stomatal) influences, as seen by comparison of the ponderosa pine and Douglas-fir forests. Other canopy-level influences that may be important are those that cause changes in photosynthetic rates such as because of changes in light level. Ecosystem-scale controls such as soil temperature and subsequent effects on belowground respiration appeared to be very important at both the wet and dry forest during the rain-free period. Therefore, we suggest that stomatal and belowground processes, both at the ecosystem scale, interact to regulate $\delta^{13}C_R$. Direct comparison of $\delta^{13}C_R$ to G_c at the ponderosa pine forest allowed us to move beyond the simplistic $\delta^{13}C_R$–climate comparisons and test a proximal mechanism.

Acknowledgements

We appreciate the extensive and strenuous field assistance of Justin Soares as well as Chun-ta Lai and Timothy Jackson. Lab assistance was provided by A. West, S. Englund, D. Galvez, T. Jensen, S. Kincaid, C. Cook, M. Lott, and S. B. Bill. Margaret Barbour graciously shared an Excel model of carbon isotope discrimination for calculation of Fig. 1b. Starker Forests Inc. (Philomath, OR, USA) provided generous access to their Douglas-fir plantations. We also appreciate enjoyable conversations with Richard Waring. This research was supported by a grant from the United States Department of Agriculture (99-35101-7772), and B. Law's and J. Irvine's support for the AmeriFlux research is from the US Department of Energy Terrestrial Carbon Program (DOE grant # FG0300ER63014). Any opinions, findings, and conclusions or recommendations expressed in this publication are those of the authors and do not necessarily reflect the views of USDA or DOE.

References

Anthoni PM, Unsworth MH, Law BE *et al.* (2002) Seasonal differences in carbon and water vapor exchange in young and old-growth ponderosa pine ecosystems. *Agricultural and Forest Meteorology*, **111**, 203–222.

Balesdent J, Girardin C, Mariotti A (1993) Site-related $\delta^{13}C$ of tree leaves and soil organic matter in a temperate forest. *Ecology*, **74**, 1713–1721.

Battle M, Bender ML, Tans PP *et al.* (2000) Global carbon sinks and their variability inferred from atmospheric O_2 and $\delta^{13}C$. *Science*, **287**, 2467–2470.

Bhupinderpal Singh, Nordgren A, Ottosson Löfvenius M *et al.* (2003) Tree root and soil heterotrophic respiration as revealed by girdling of boreal Scots pine forest: extending observations beyond the first year. *Plant, Cell and Environment*, **26**, 1287–1296.

Bowling DR, Cook CS, Ehleringer JR (2001) Technique to measure CO_2 mixing ratio in small flasks with a bellow/IRGA system. *Agricultural and Forest Meteorology*, **109**, 61–65.

Bowling DR, McDowell NG, Bond BJ *et al*. (2002) ^{13}C content of ecosystem respiration is linked to precipitation and vapor pressure deficit. *Oecologia*, **131**, 113–124.

Bowling D, McDowell NG, Welker JM *et al*. (2003) Oxygen isotope content of CO_2 in nocturnal ecosystem respiration: 1. Observations in forests along a precipitation transect in Oregon, USA. *Global Biogeochemical Cycles*, **17**, d.o.i. 10.1029/2001GB002082.

Brooks JR, Meinzer FC, Coulombe R *et al*. (2002) Hydraulic redistribution of soil water during summer drought in two contrasting Pacific Northwest coniferous forests. *Tree Physiology*, **22**, 1107–1117.

Brugnoli E, Farquhar GD (2000) Photosynthetic fractionation of carbon isotopes. In: *Photosynthesis: Physiology and Metabolism*, **Vol. 9** (eds Leegood RC, Sharkey TD, von Caemmerer S), Kluwer Academic, the Netherlands.

Brugnoli E, Scartazza A, Lauteri M *et al*. (1998) Carbon isotope discrimination in structural and non-structural carbohydrates in relation to productivity and adaptation to unfavourable conditions. In: *Stable Isotopes* (ed. Griffiths H), pp. 133–146. BIOS Scientific Publishers, Limited, Oxford.

Buchmann N, Brooks JR, Flanagan LB *et al*. (1998) Carbon isotope discrimination by terrestrial ecosystems. In: *Stable Isotopes* (ed. Griffiths H), pp. 203–222. BIOS Scientific Publishers, Limited, Oxford.

Canadell JG, Mooney HA, Baldocchi DD *et al*. (2000) Carbon metabolism of the terrestrial biosphere: a multitechnique approach for improved understanding. *Ecosystems*, **3**, 115–130.

Cerling TE, Solomon DK, Quade J *et al*. (1991) On the isotopic composition of carbon in soil carbon dioxide. *Geochimica et Cosmochimica Acta*, **55**, 3403–3405.

Ciais P, Friedlingstein P, Schimel DS *et al*. (1999) A global calculation of the $\delta^{13}C$ of soil respired carbon: implications for the biospheric uptake of anthropogenic CO_2. *Global Biogeochemical Cycles*, **13**, 519–530.

Ciais P, Tans PP, Trolier M *et al*. (1995) A large northern hemisphere terrestrial CO_2 sink indicated by the $^{13}C/^{12}C$ ratio of atmospheric CO_2. *Science*, **269**, 1089–1102.

Ehleringer JR, Buchmann N, Flanagan LB (2000) Carbon isotope ratios in belowground carbon cycle processes. *Ecological Applications*, **10**, 412–422.

Ehleringer JR, Cook CS (1998) Carbon and oxygen isotope ratios of ecosystem respiration along an Oregon conifer transect: preliminary observations based on small-flask sampling. *Tree Physiology*, **18**, 513–519.

Ehleringer JR, Hall AE, Farquhar GD (1993) *Stable Isotopes and Plant Carbon–Water Relations*. Academic Press, San Diego, CA.

Ekblad A, Högberg P (2001) Natural abundance of ^{13}C in CO_2 respired from forest soils reveals speed of link between tree photosynthesis and root respiration. *Oecologia*, **127**, 305–308.

Enquist BJ, Economo EP, Huxman TE *et al*. (2003) Scaling metabolism from organisms to ecosystems. *Nature*, **423**, 639–642.

Farquhar GD, Ehleringer JR, Hubick KT (1989) Carbon isotope discrimination and photosynthesis. *Annual Review of Plant Physiology and Plant Molecular Biology*, **40**, 503–537.

Fessenden JE, Ehleringer JR (2003) Temporal variation in $\delta^{13}C_R$ of ecosystem respiration in the Pacific Northwest: links to moisture stress. *Oecologia*, **136**, 129–136.

Fernandez I, Mahieu N, Cadisch G (2003) Carbon isotopic fractionation during decomposition of plant materials of different quality. *Global Biogeochemical Cycles*, **17**, doi:10.1029/2001GB001834.

Flanagan LB, Ehleringer JR (1998) Ecosystem-atmosphere CO_2 exchange: interpreting signals of change using stable isotope ratios. *Trends in Ecology and Evolution*, **13**, 10–14.

Fung I, Field CB, Berry JA *et al*. (1997) Carbon 13 exchanges between the atmosphere and biosphere. *Global Biogeochemical Cycles*, **11**, 507–533.

Ghashgaie J, Badeck F-W, Lanigan G *et al*. (2003) Carbon isotope fractionation during dark respiration and photorespiration in C_3 plants. *Phytochemistry Reviews*, **2**, 145–161.

Högberg P, Plamboeck AH, Taylor AFS *et al*. (1999) Natural ^{13}C abundance reveals trophic status of fungi and host-origin of carbon in mycorrhizal fungi in mixed forests. *Proceedings of the National Academy of Science of the USA*, **96**, 8534–8539.

Högberg P, Nordgren A, Buchmann N *et al*. (2001) Large-scale forest girdling shows that current photosynthesis drives soil respiration. *Nature*, **411**, 789–792.

Hubbard RM, Bond BJ, Ryan MG (1999) Evidence that hydraulic conductance limits photosynthesis in old *Pinus ponderosa* trees. *Tree Physiology*, **19**, 165–172.

Irvine J, Law BE (2002) Seasonal soil CO_2 effluxes in young and old ponderosa pine forests. *Global Change Biology*, **8**, 1183–1194.

Irvine J, Law BE, Anthoni PM (2002) Water limitations to carbon exchange in old-growth and young ponderosa pine stands. *Tree Physiology*, **22**, 189–196.

Jarvis PG, McNaughton KG (1986) Stomatal control of transpiration: scaling up from leaf to region. *Advances in Ecological Research*, **15**, 1–49.

Kaufmann MR (1976) Stomatal responses of Engelmann spruce to humidity, light, and water stress. *Plant Physiology*, **57**, 898–901.

Keeling CD (1958) The concentration and isotopic abundances of atmospheric carbon dioxide in rural areas. *Geochimica et Cosmochimica Acta*, **13**, 322–334.

Kelliher FM, Ross DJ, Law BE *et al*. (2004) Carbon and nitrogen mineralization in litter and mineral soil of young and old ponderosa pine forests during summer drought and after wetting. *Forest Ecology and Management*, **191**, 201–213.

Lai C-T, Ehleringer JR, Wofsy SC *et al*. (2004) Estimating photosynthetic ^{13}C discrimination in terrestrial CO_2 exchange from canopy to regional scales. *Global Biogeochemical Cycles*, d.o.i. 10.1029/2003GB002148.

Law BE, Ryan MG, Anthoni PM (1999) Seasonal and annual respiration of a ponderosa pine ecosystem. *Global Change Biology*, **5**, 169–182.

Law BE, Sun OJ, Campbell J *et al*. (2003) Changes in carbon storage and fluxes in a chronosequence of ponderosa pine. *Global Change Biology*, **9**, 510–524.

Law BE, Thornton P, Irvine J *et al*. (2001) Carbon storage and fluxes in ponderosa pine forests at different developmental stages. *Global Change Biology*, **7**, 755–777.

Lin G, Ehleringer JR (1997) Carbon isotopic fractionation does not occur during dark respiration in C_3 and C_4 plants. *Plant Physiology*, **114**, 391–394.

Lloyd J, Farquhar GD (1994) ^{13}C discrimination during CO$_2$ assimilation by the terrestrial biosphere. *Oecologia*, **99**, 201–215.

Marshall JD, Rehfeldt GE, Monserud RA (2001) Family differences in height growth and photosynthetic traits in three conifers. *Tree Physiology*, **21**, 727–734.

McDowell NG, Balster N, Marshall JD (2001) Belowground carbon allocation of Rocky Mountain Douglas-fir. *Canadian Journal of Forest Research*, **31**, 1425–1436.

McDowell NG, Bowling DR, Bond BJ *et al*. (2004) Response of the carbon isotope content of ecosystem, leaf and soil respiration to meteorological and physiological driving factors in a *Pinus ponderosa* ecosystem. *Global Biogeochemical Cycles*, **16**, d.o.i. 10.1029/2003GB002049.

McDowell NG, Phillips N, Lunch CK *et al*. (2002) Hydraulic limitation and compensation in large, old Douglas-fir trees. *Tree Physiology*, **22**, 763–774.

Miller JB, Tans PP (2003) Calculating isotopic fractionation from isotopic measurements at various scales. *Tellus*, **55B**, 207–214.

Mortazavi B, Chanton JP (2002) Carbon isotopic discrimination and control of nighttime canopy δ^{18}O–CO$_2$ in a pine forest in the southeastern United States. *Global Biogeochemical Cycles*, **16**, d.o.i. 10.1029/2001GB001390.

Nadelhoffer KJ, Fry B (1988) Controls on natural nitrogen-15 and carbon-13 abundances in forest soil organic matter. *Soil Science Society of America Journal*, **52**, 1633–1640.

Ometto JPHB, Flanagan LB, Martinelli LA *et al*. (2002) Carbon isotope discrimination in forest and pasture ecosystems of the Amazon Basin, Brazil. *Global Biogeochemical Cycles*, **16**, d.o.i. 10.1029/2001GB001462.

Oquist G, Huner NPA (2003) Photosynthesis of overwintering evergreen plants. *Annual Review of Plant Biology*, **54**, 329–355.

Pataki DE, Ehleringer JR, Flanagan LB *et al*. (2003) The application and interpretation of Keeling plots in terrestrial carbon cycle research. *Global Biogeochemical Cycles*, **17**, d.o.i. 10.1029/2001GB001850.

Paul EA, Clark FE (1989) *Soil Microbiology and Biochemistry*. Academic Press Inc., San Diego, CA.

Randerson JT, Collatz GJ, Fessenden JE *et al*. (2002a) A possible global covariance between terrestrial gross primary production and ^{13}C discrimination: consequences for the atmospheric ^{13}C budget and its response to ENSO. *Global Biogeochemical Cycles*, **16**, d.o.i. 10.1029/2001GB001435.

Randerson JT, Still CJ, Balle JJ *et al*. (2002b) Carbon isotope discrimination of arctic and boreal biomes inferred from remote atmospheric measurements and a biosphere–atmosphere model. *Global Biogeochemical Cycles*, **16**, d.o.i. 10.1029/2001GB001845.

Schauer AJ, Lai C-T, Bowling DR *et al*. (2003) An automated sampler for collection of atmospheric trace gas samples for stable isotope analyses. *Agricultural and Forest Meteorology*, **118**, 113–124.

Schnyder H, Schäufele R, Lötscher M *et al*. (2003) Disentangling CO$_2$ fluxes: direct measurements of mesocosm-scale natural abundance ^{13}CO$_2$/^{12}CO$_2$ gas exchange, ^{13}C discrimination, and labelling of CO$_2$ exchange flux components in controlled environments. *Plant, Cell and Environment*, **26**, 1863–1874.

Schönwitz R, Stichler W, Ziegler H (1986) δ^{13}C values of CO$_2$ from soil respiration on sites with crops of C$_3$ and C$_4$ type of photosynthesis. *Oecologia*, **69**, 305–308.

Schulze E-D, Mooney HA, Sala OE *et al*. (1998) Carbon and nitrogen isotope discrimination and nitrogen nutrition of trees along a rainfall gradient in northern Australia. *Australian Journal of Plant Physiology*, **25**, 413–425.

Smith WK, Young DR, Carter GA *et al*. (1984) Autumn stomatal closure in six conifer species of the Central Rocky Mountains. *Oecologia*, **63**, 237–242.

Sokal RR, Rohlf FJ (1995) *Biostatistics*. W. H. Freeman and Co., New York.

Strand M, Lundmark T, Söderbergh I *et al*. (2002) Impacts of seasonal air and soil temperatures on photosynthesis in Scots pine trees. *Tree Physiology*, **22**, 839–847.

Tans PP (1980) On calculating the transfer of carbon-13 in reservoir models of the carbon cycle. *Tellus*, **32**, 464–469.

Taylor GH, Hannan C (1999) *The Climate of Oregon*. Oregon State University Press, Corvallis, OR, USA.

Tcherkez G, Nogués S, Bleton J *et al*. (2003) Metabolic origin of carbon isotope composition of leaf dark-respired CO$_2$ in French bean. *Plant Physiology*, **131**, 237–244.

Weiskittel AR (2003) *Alterations in Douglas-fir crown structure, morphology and dynamics imposed by the Swiss Needle Cast disease in the Oregon Coast Range*. MSc thesis, Department of Forest Resources, Oregon State University, 409pp.

Williams M, Law BE, Anthoni PM *et al*. (2001) Using a simulation model and ecosystem flux data to examine carbon-water interactions in ponderosa pine. *Tree Physiology*, **21**, 287–298.

Wilson KB, Baldocchi DD, Hanson PJ (2001) Leaf age affects the seasonal pattern of photosynthetic capacity and net ecosystem exchange of carbon in a deciduous forest. *Plant, Cell and Environment*, **24**, 571–583.

Yoder BJ, Ryan MG, Waring RH *et al*. (1994) Evidence of reduced photosynthetic rates in old trees. *Forest Science*, **40**, 513–527.

Zimmerman JK, Ehleringer JR (1990) Carbon isotope ratios are correlated with irradiance levels in the Panamanian orchid *Catasetum viridiflavum*. *Oecologia*, **83**, 247–249.